Inversion for indicators of interconnected / aligned cracks

Joint PP and PS AVAZ inversion for orthogonal fracture weaknesses

Huaizhen Chen and Kris Innanen

Calgary, AB, Canada

December 3, 2020

Outline

- Introduction
- Theory and method
- Numerical examples
- Conclusions

Introduction

- Assumption of single set of fractures

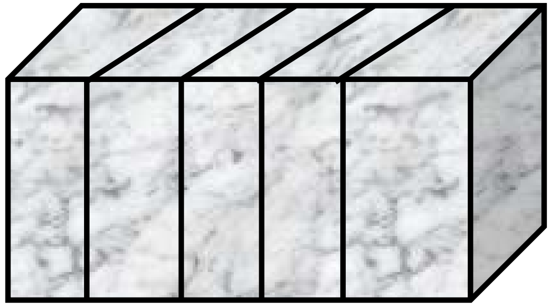

HTI media

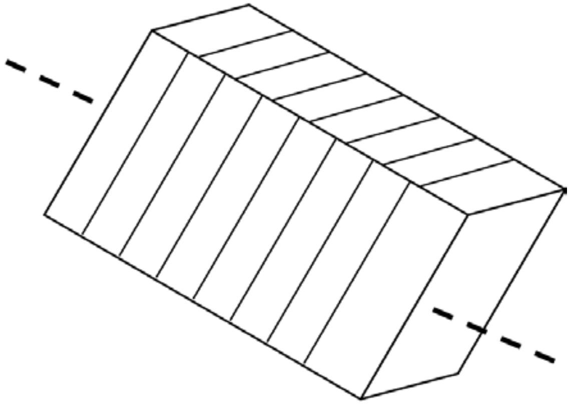

TTI media

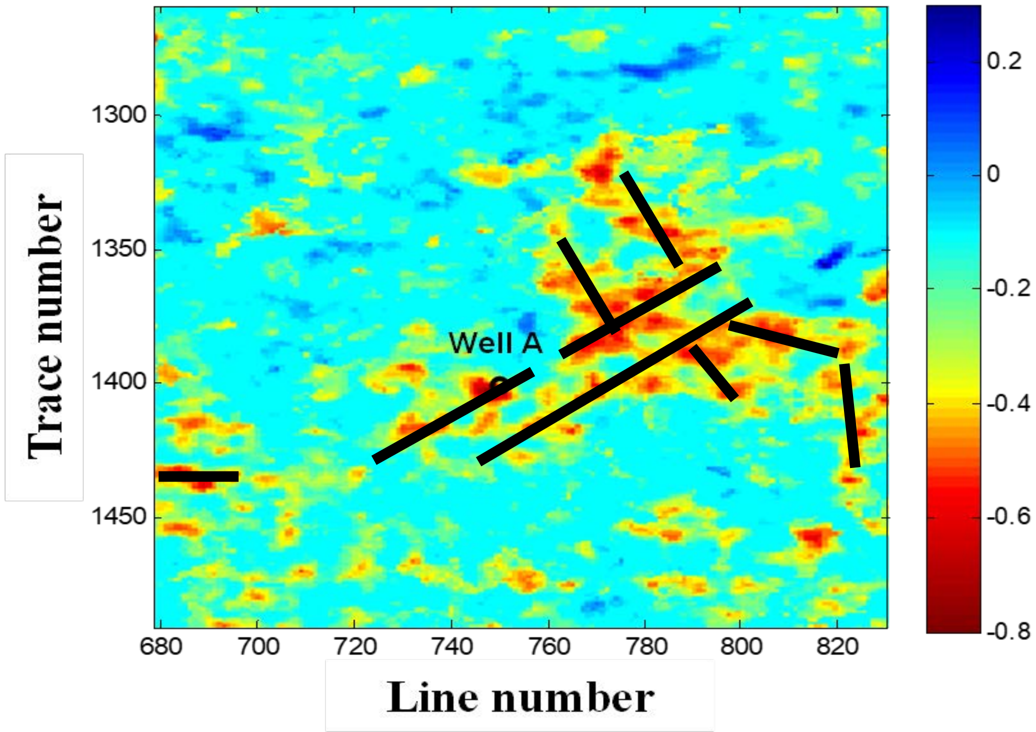

Fracture connectivity?

Introduction

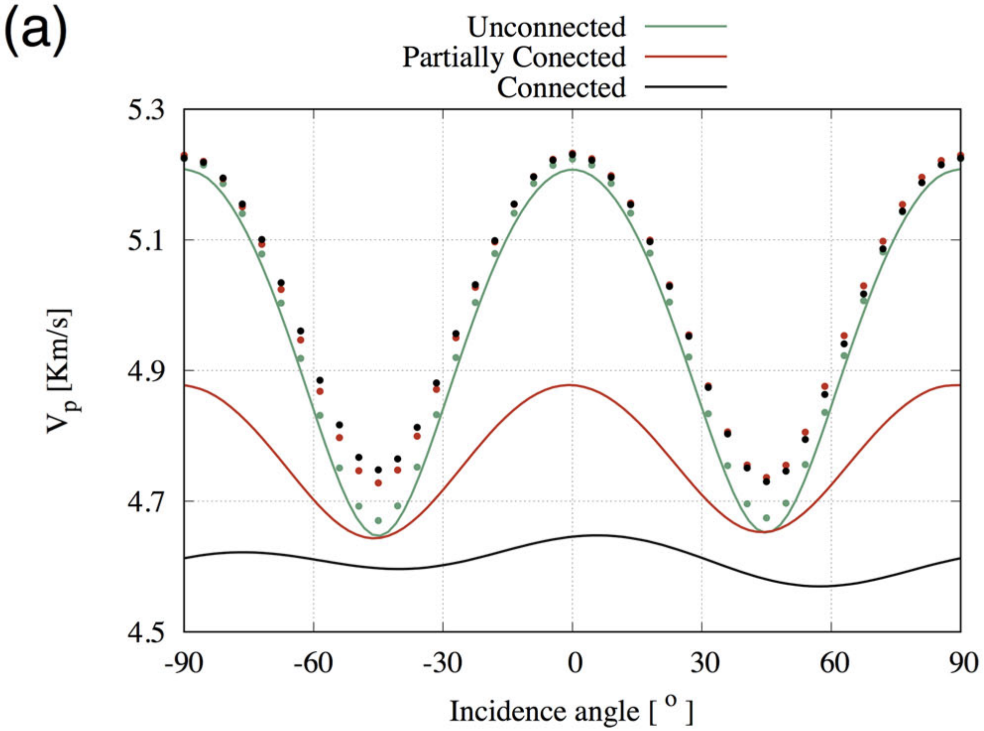

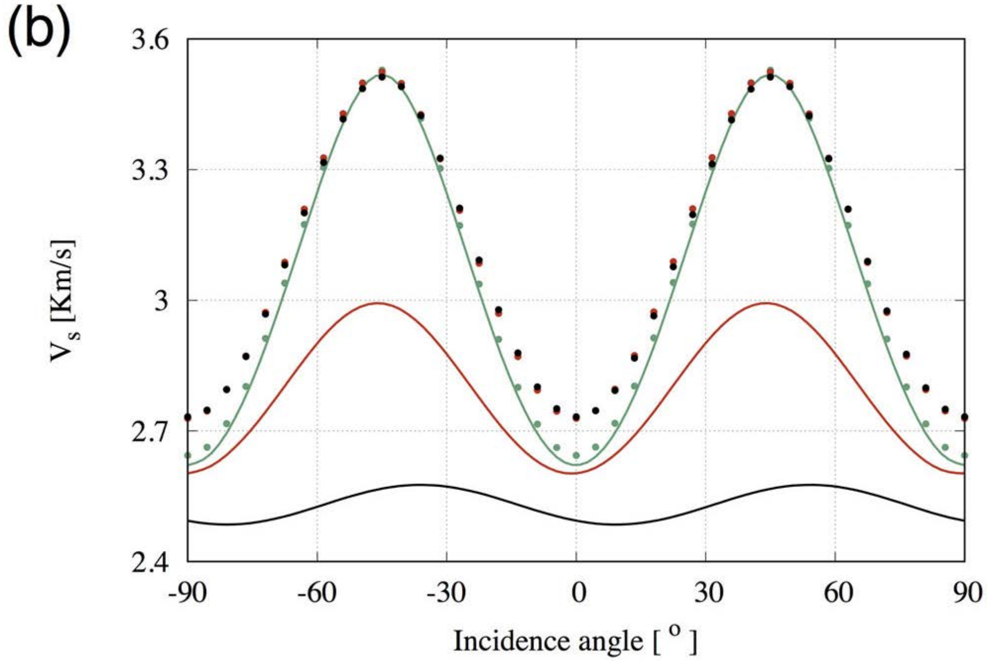

Fracture connectivity can reduce the velocity anisotropy of seismic waves.
(Rubino et al., GJI, 2017, 210, 223–227)

How is reflection coefficient influenced by connected fractures?

Objective

- PP- and PS-wave reflection coefficients in rocks containing interconnected fractures

- Azimuthal AVO inversion for interconnected fracture indicators

Theory and method: PP- and PS-wave reflection coefficients

An effective model of two orthogonal fractures in an isotropic background

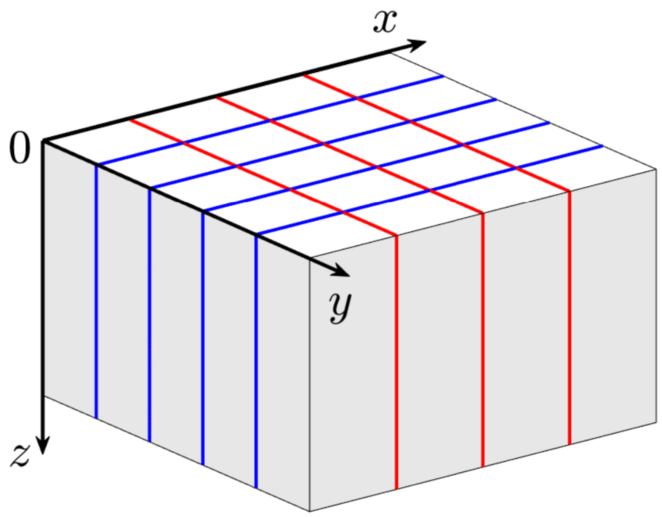

$$\mathbf{C} = \begin{bmatrix} C_{11} & C_{12} & C_{13} & 0 & 0 & 0 \\ C_{12} & C_{22} & C_{23} & 0 & 0 & 0 \\ C_{13} & C_{23} & C_{33} & 0 & 0 & 0 \\ 0 & 0 & 0 & C_{44} & 0 & 0 \\ 0 & 0 & 0 & 0 & C_{55} & 0 \\ 0 & 0 & 0 & 0 & 0 & C_{66} \end{bmatrix}$$

$$C_{11} \approx M \left[1 - \underline{\delta_{N1}} - (1-2g)^2 \underline{\delta_{N2}}\right],$$

$$C_{12} \approx \lambda \left(1 - \delta_{N1} - \delta_{N2}\right),$$

$$C_{13} \approx \lambda \left[1 - \delta_{N1} - (1-2g)\, \delta_{N2}\right],$$

$$C_{22} \approx M \left[1 - (1-2g)^2 \delta_{N1} - \delta_{N2}\right],$$

$$C_{23} \approx \lambda \left[1 - (1-2g)\, \delta_{N1} - \delta_{N2}\right],$$

$$C_{33} \approx M \left[1 - (1-2g)^2 \delta_{N1} - (1-2g)^2 \delta_{N2}\right],$$

$$C_{44} = \mu \left(1 - \delta_{T2}\right),$$

$$C_{55} = \mu \left(1 - \delta_{T1}\right),$$

$$C_{66} \approx \mu \left(1 - \underline{\delta_{T1}} - \underline{\delta_{T2}}\right).$$

Theory and method: PP- and PS-wave reflection coefficients

An interface separating an isotropic medium and a medium with two orthogonal fractures

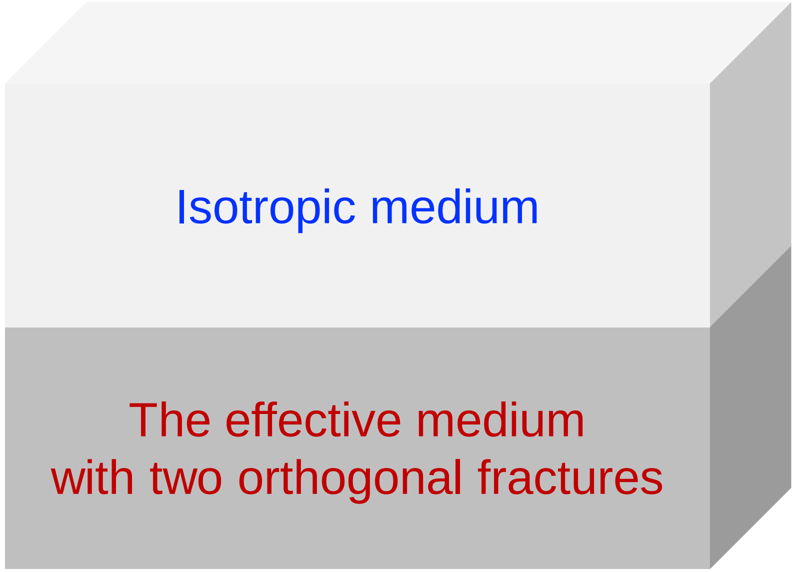

$$R_{\mathrm{PP}}(\theta,\phi) = R_{\mathrm{PP}}^{\mathrm{iso}}(\theta) + R_{\mathrm{PP}}^{\mathrm{ani}}(\theta,\phi),$$

$$R_{\mathrm{PS}}(\theta,\phi) = R_{\mathrm{PS}}^{\mathrm{iso}}(\theta) + R_{\mathrm{PS}}^{\mathrm{ani}}(\theta,\phi)$$

Isotropic part

$$R_{\mathrm{PP}}^{\mathrm{iso}}(\theta) = a_\rho(\theta)\frac{\Delta\rho}{\rho} + a_M(\theta)\frac{\Delta M}{M} + a_\mu(\theta)\frac{\Delta\mu}{\mu},$$

$$R_{\mathrm{PS}}^{\mathrm{iso}}(\theta) = b_\mu(\theta)\frac{\Delta\mu}{\mu} + b_\rho(\theta)\frac{\Delta\rho}{\rho}$$

Anisotropic part

$$\begin{aligned} R_{\mathrm{PP}}^{\mathrm{ani}}(\theta,\phi) = {} & a_{N1}(\theta,\phi)\delta_{N1} + a_{N2}(\theta,\phi)\delta_{N2} \\ & + a_{T1}(\theta,\phi)\delta_{T1} + a_{T2}(\theta,\phi)\delta_{T2}, \end{aligned}$$

$$\begin{aligned} R_{\mathrm{PS}}^{\mathrm{ani}}(\theta,\phi) = {} & b_{N1}(\theta,\phi)\,\delta_{N1} + b_{N2}(\theta,\phi)\,\delta_{N2} \\ & + b_{T1}(\theta,\phi)\,\delta_{T1} + b_{T2}(\theta,\phi)\,\delta_{T2}, \end{aligned}$$

Theory and method: PP- and PS-wave reflection coefficients

Assumptions for simplifying two sets of fracture weaknesses

$$\delta_{N1} = \frac{4e_1}{3g(1-g)\left[1+\frac{1}{\pi g(1-g)}\frac{K_{f1}}{\mu\chi_1}\right]},$$

$$\delta_{T1} = \frac{16e_1}{3(3-2g)},$$

$$\delta_{N2} = \frac{4e_2}{3g(1-g)\left[1+\frac{1}{\pi g(1-g)}\frac{K_{f2}}{\mu\chi_2}\right]},$$

$$\delta_{T2} = \frac{16e_2}{3(3-2g)},$$

1) The same infilling fluids

$$K_f = K_{f1} = K_{f2}$$

2) The approxiamtely equal aspect ratio

$$\chi \approx \chi_1 \approx \chi_2$$

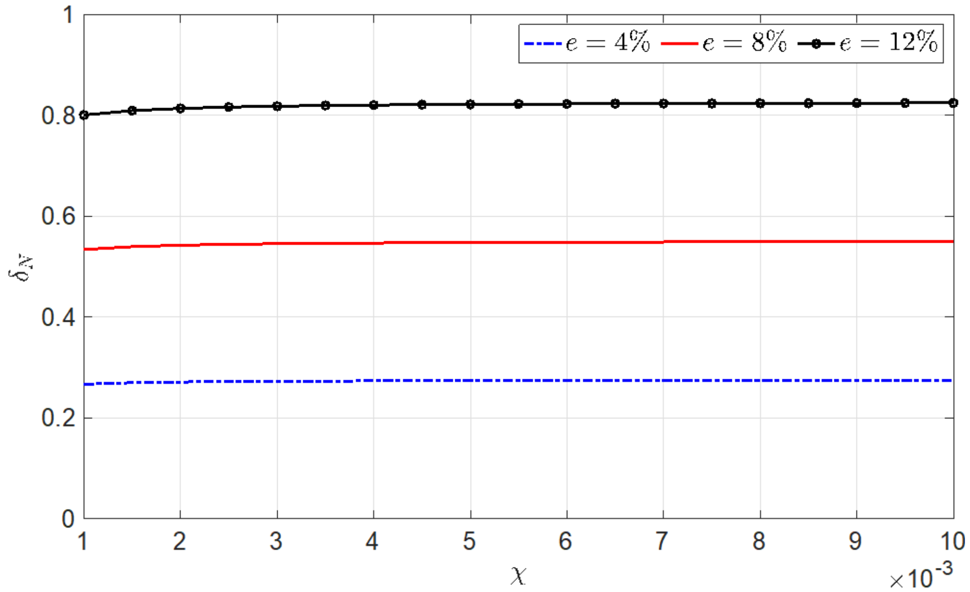

$$\delta_{N1} = \gamma\delta_{N2},$$
$$\delta_{T1} = \gamma\delta_{T2},$$
$$\gamma = \frac{e_1}{e_2}$$

Theory and method: PP- and PS-wave reflection coefficients

	δ_{N1}	δ_{T1}	δ_{N2}	δ_{T2}
Sand	0	0	0	0
Shale (one set)	0	0	0.7849	0.3183
Shale (two sets)	0.1047	0.0424	0.7849	0.3183

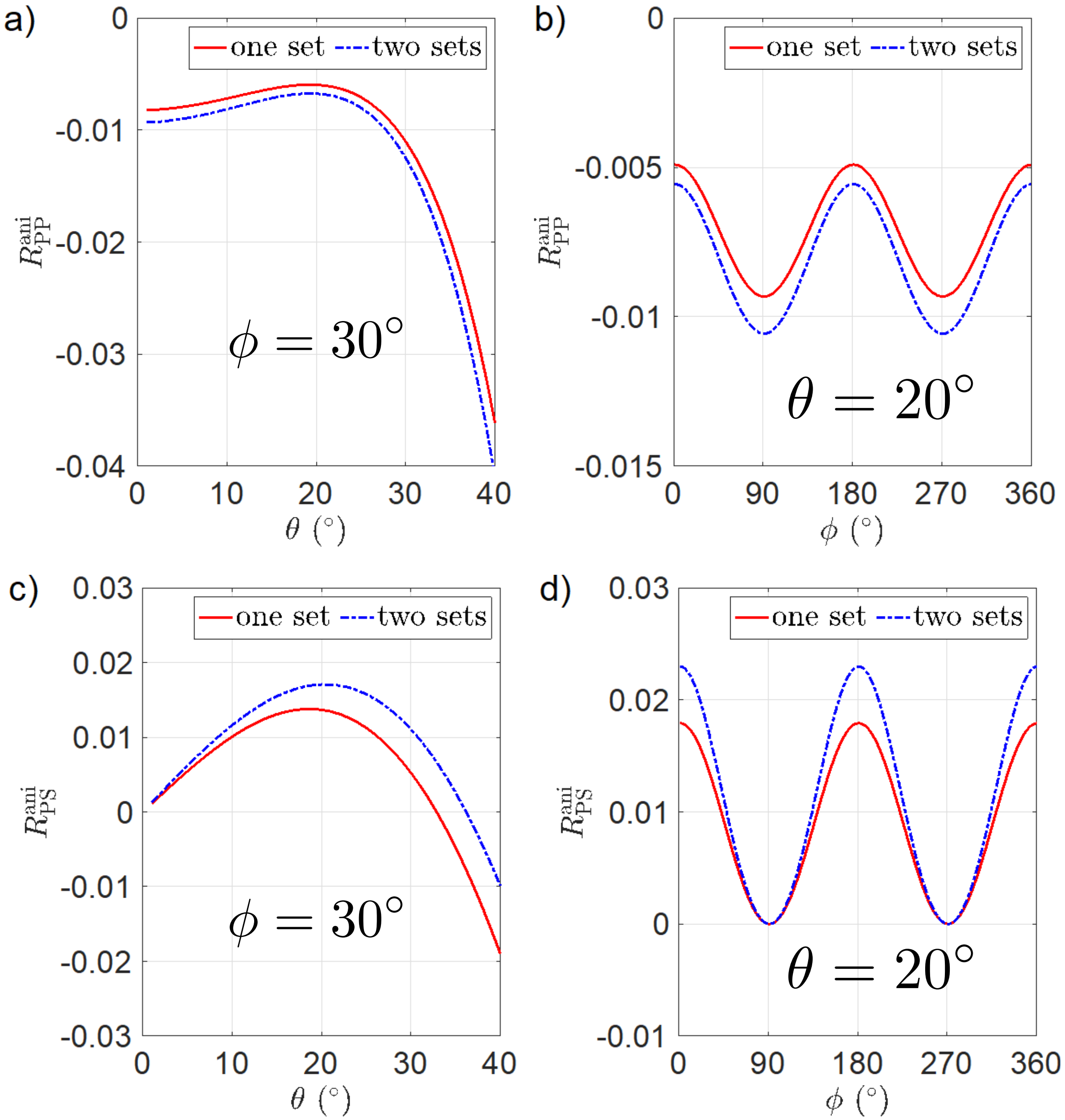

PP-wave

PS-wave

Theory and method: Bayesian MCMC inversion approach

Input datasets:

Differences in azimuthal reflection coefficients variation with incidence angle

$$\Delta R_{\mathrm{PP}}(\theta,\phi_1,\phi_k) = \mathcal{P}_N(\theta,\phi_1,\phi_k)\,\delta_{N2} + \mathcal{P}_T(\theta,\phi_1,\phi_k)\,\delta_{T2},$$

$$\Delta R_{\mathrm{PS}}(\theta,\phi_1,\phi_k) = \mathcal{Q}_N(\theta,\phi_1,\phi_k)\,\delta_{N2} + \mathcal{Q}_T(\theta,\phi_1,\phi_k)\,\delta_{T2},$$

Workflow

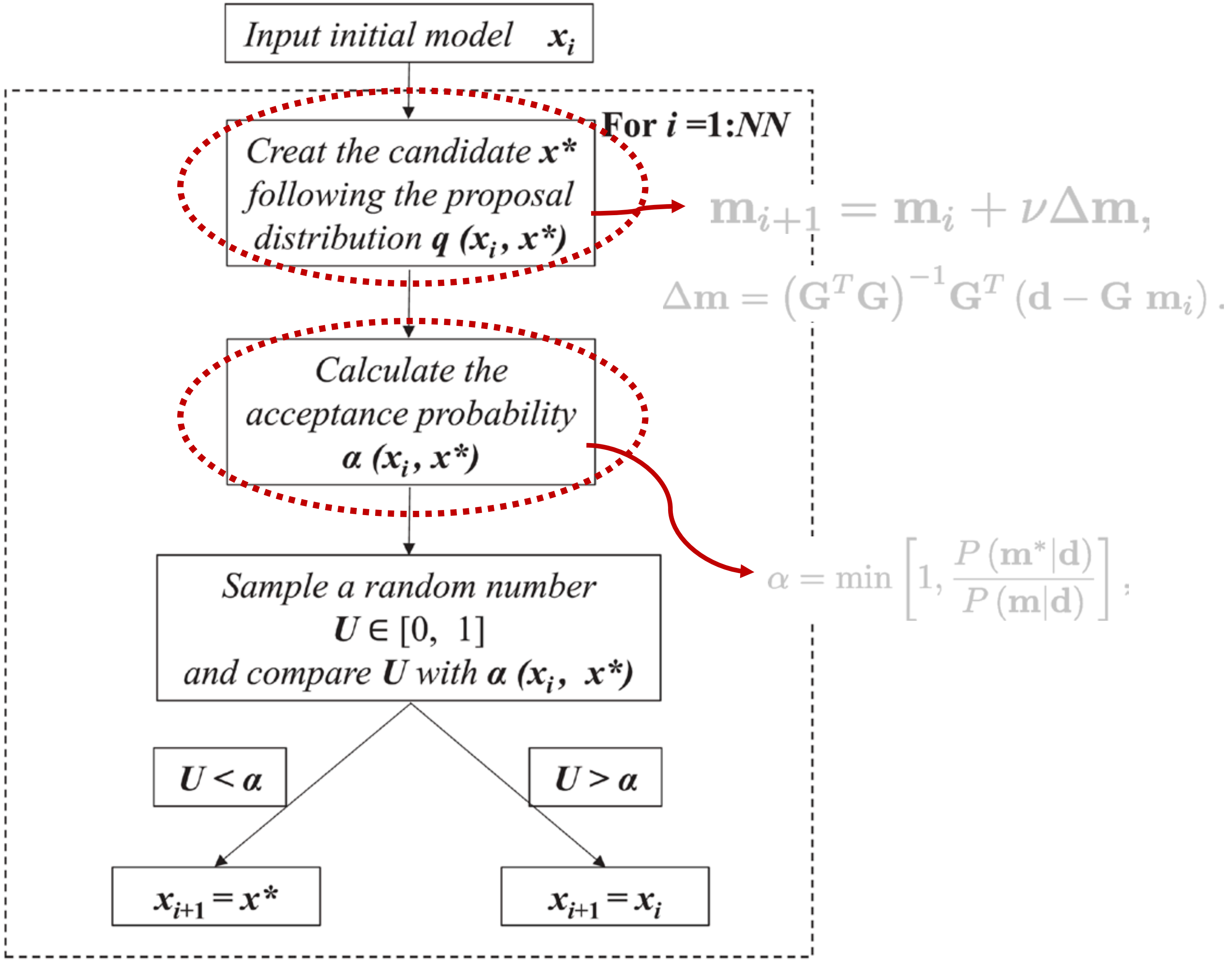

Theory and method: Bayesian MCMC inversion approach

Posterior PDF

$$P(\mathbf{m}|\mathbf{d}) \propto P(\mathbf{d}|\mathbf{m}) P(\mathbf{m})$$

$$\propto \exp\left(-\frac{(\mathbf{d}-\mathbf{Gm})^T(\mathbf{d}-\mathbf{Gm})}{2\sigma_{\mathrm{noise}}^2}\right) \exp\left(-\frac{(\mathbf{m}-m_{\mathrm{a}})^T(\mathbf{m}-m_{\mathrm{a}})}{2\sigma_{\mathbf{m}}^2}\right)$$

Gaussian random noise

Gaussian priori

Numerical examples

Curves of two fracture density and water saturation

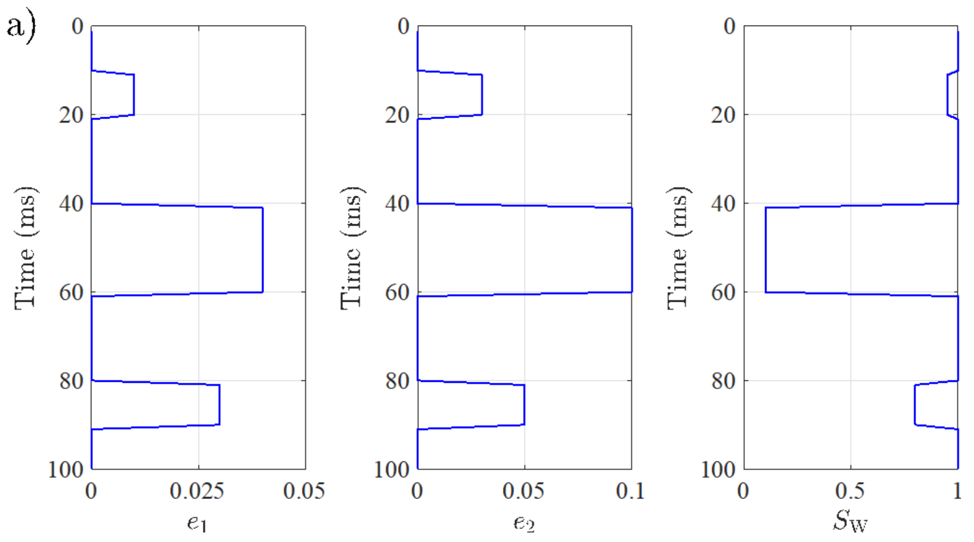

Calculated fracture weaknesses

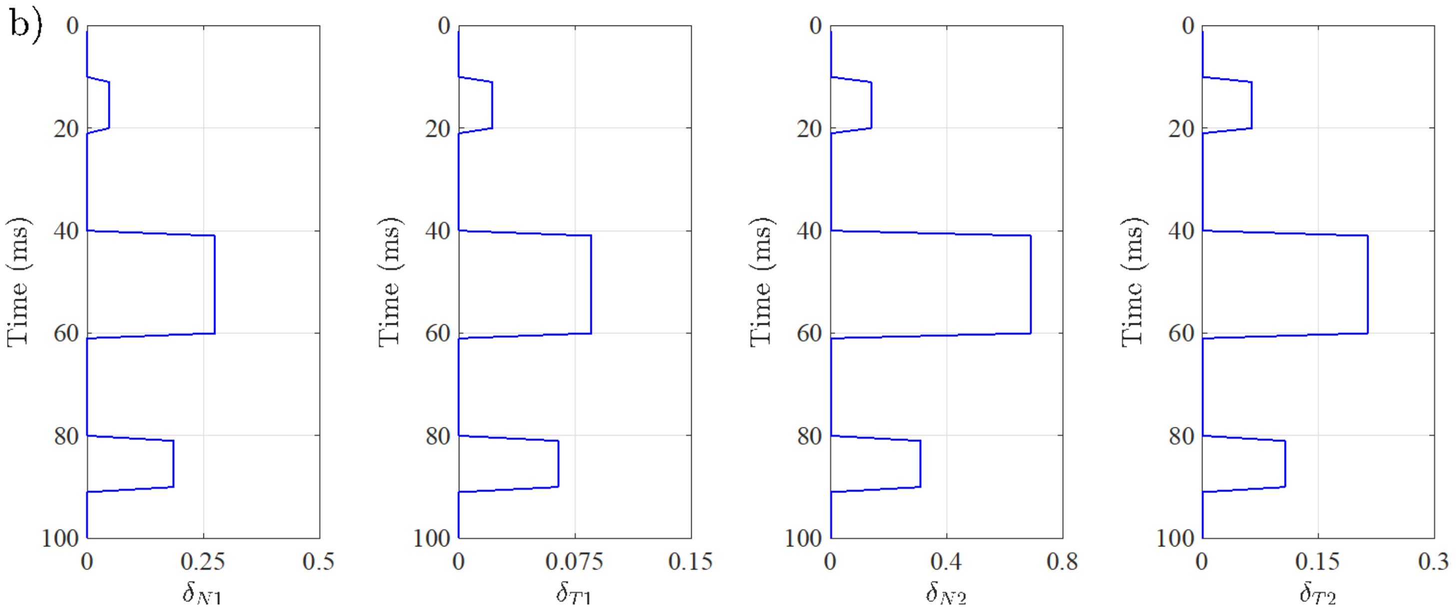

Numerical examples

Noisy synthetic seismic data

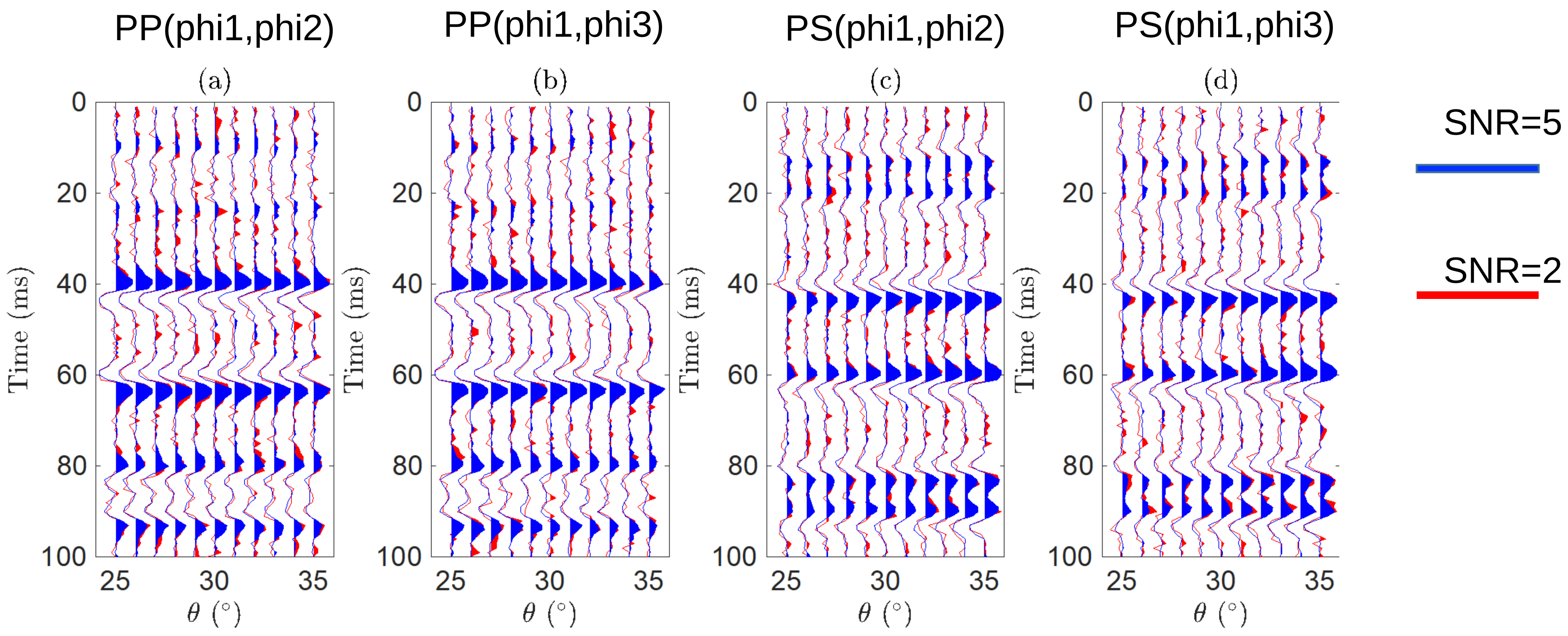

$$\phi_1 = 0^\circ, \phi_2 = 45^\circ, \phi_3 = 90^\circ$$

Numerical examples

SNR=5

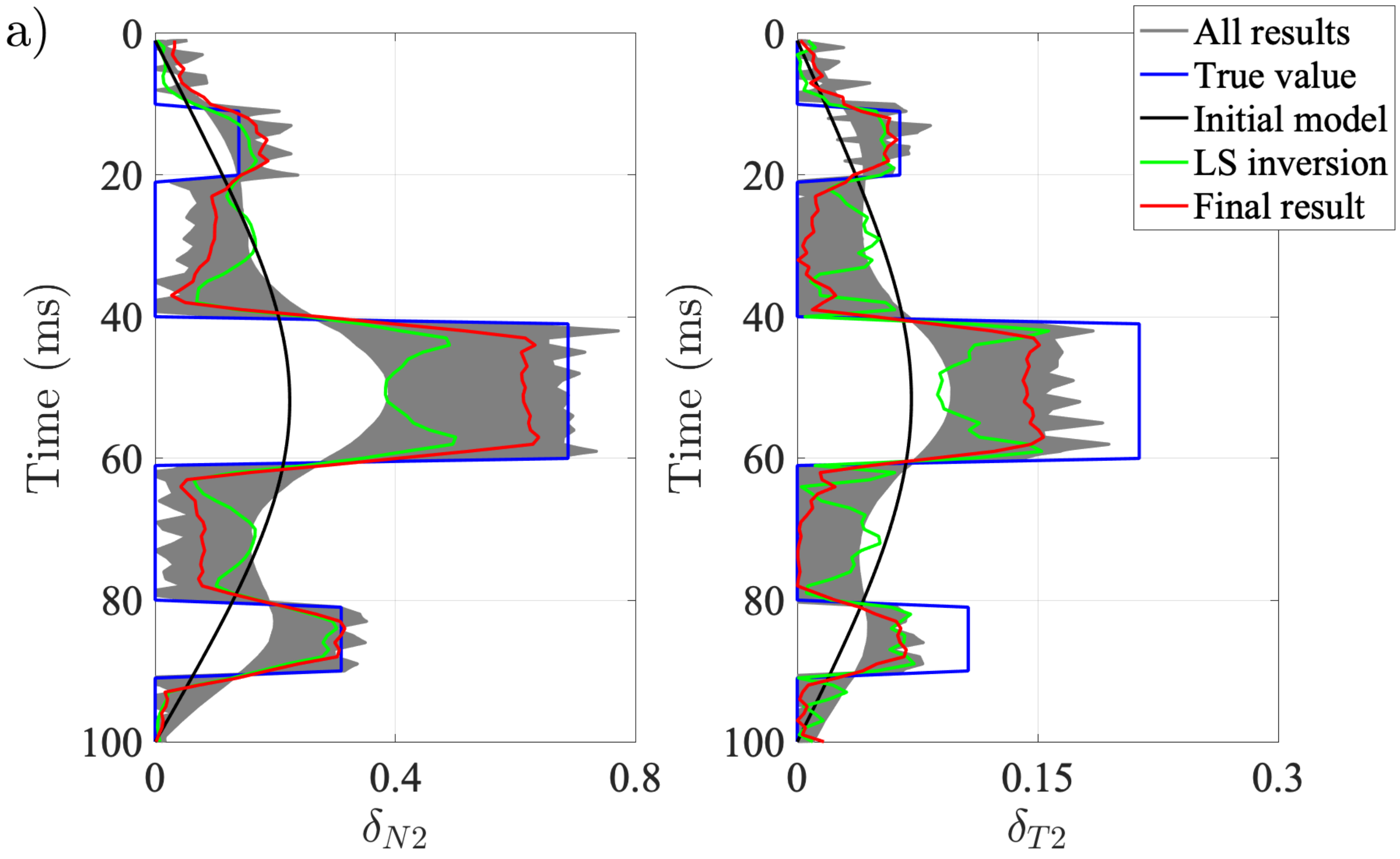

Numerical examples

SNR=2

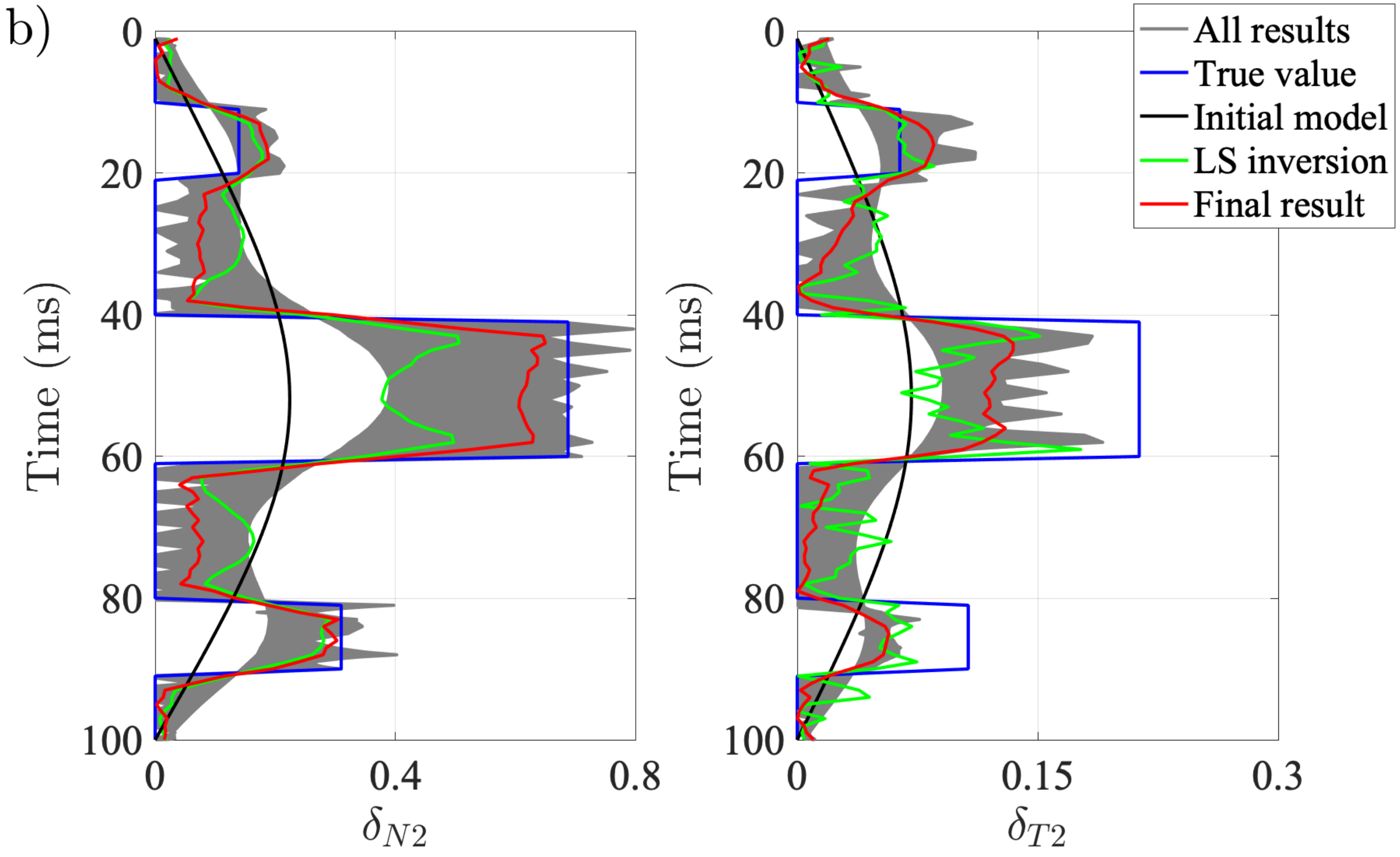

Real datasets

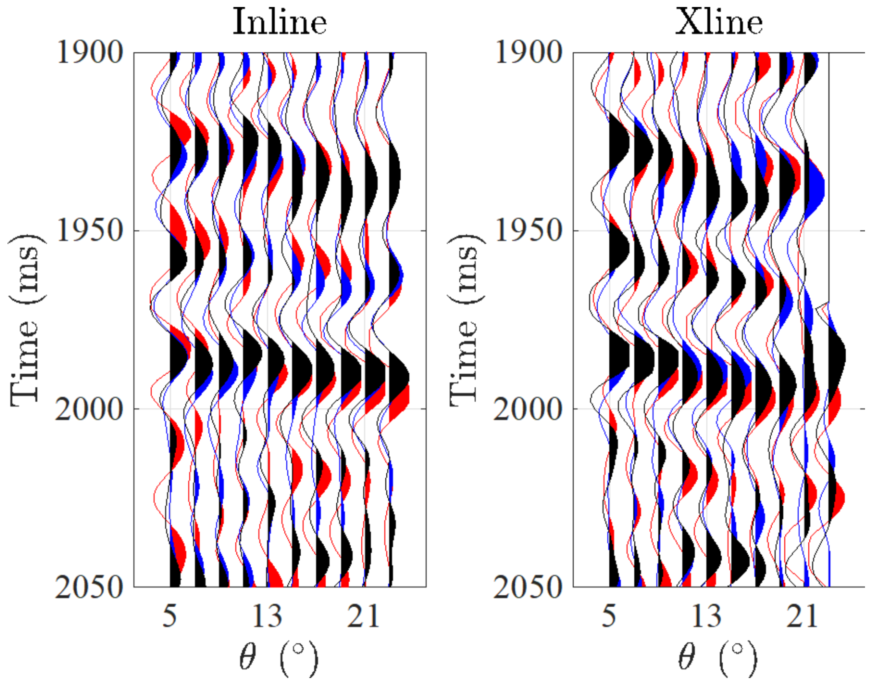

$\phi_1 = 170^\circ$ $\phi_2 = 25^\circ$ $\phi_3 = 50^\circ$

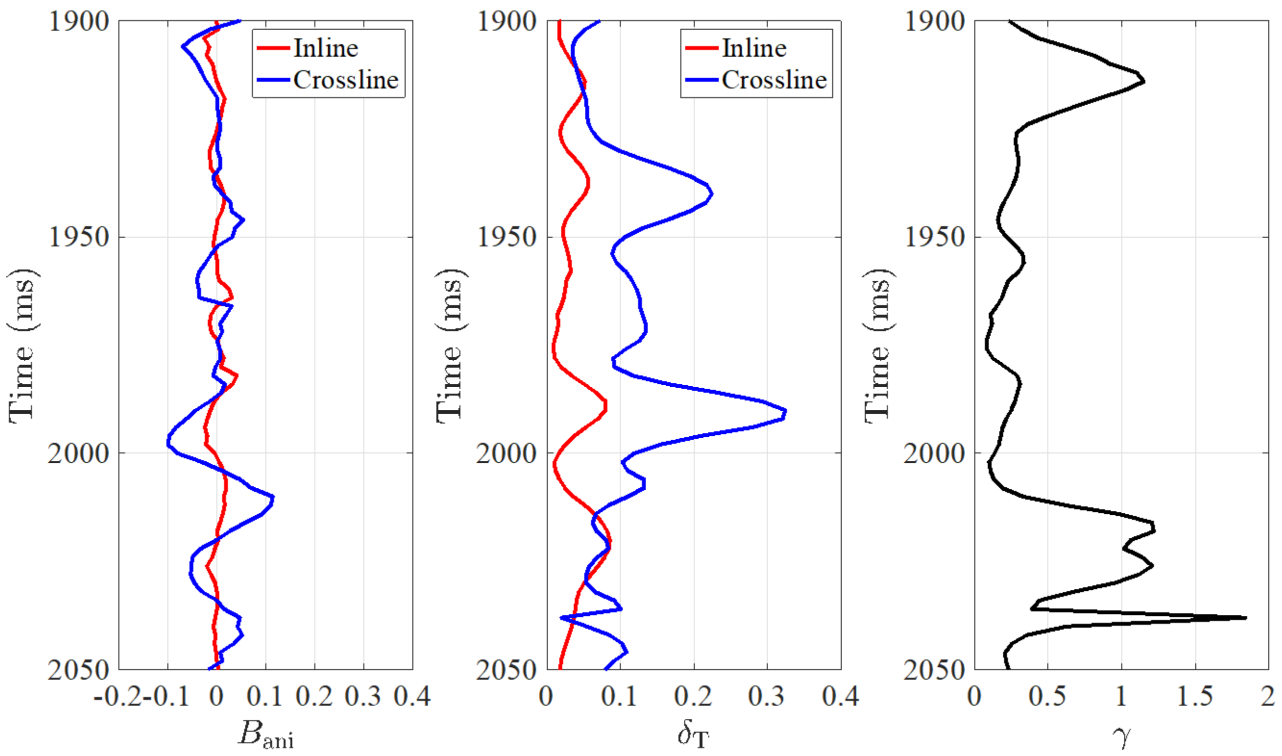

$$B_{\mathrm{ani}} \approx -g\,(1-2g)\,\delta_N + g\delta_T$$

$$\delta_N \approx \frac{3-2g}{4g\,(1-g)}\delta_T$$

Numerical examples

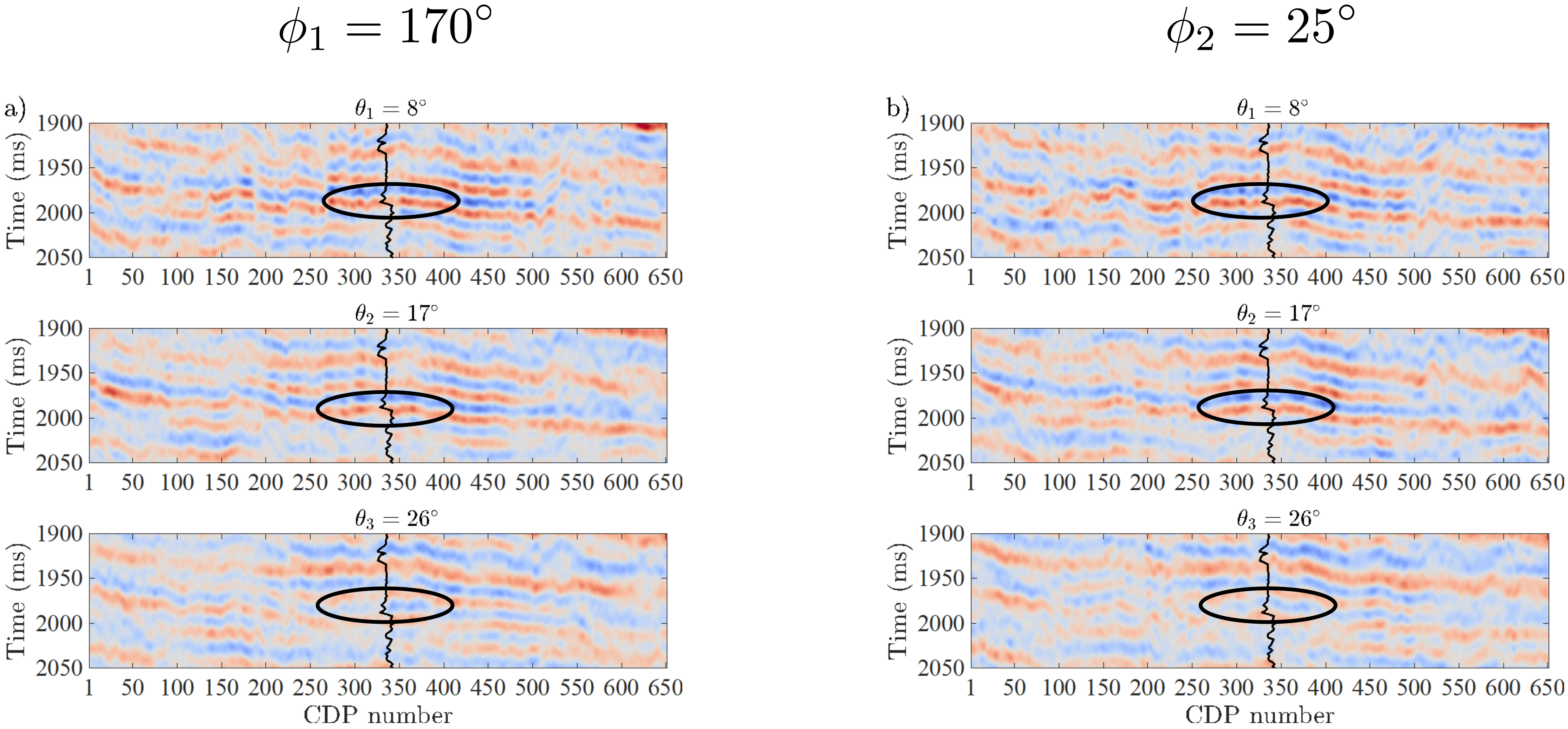

PP-wave stacked data of small, middle and large angles

Numerical examples

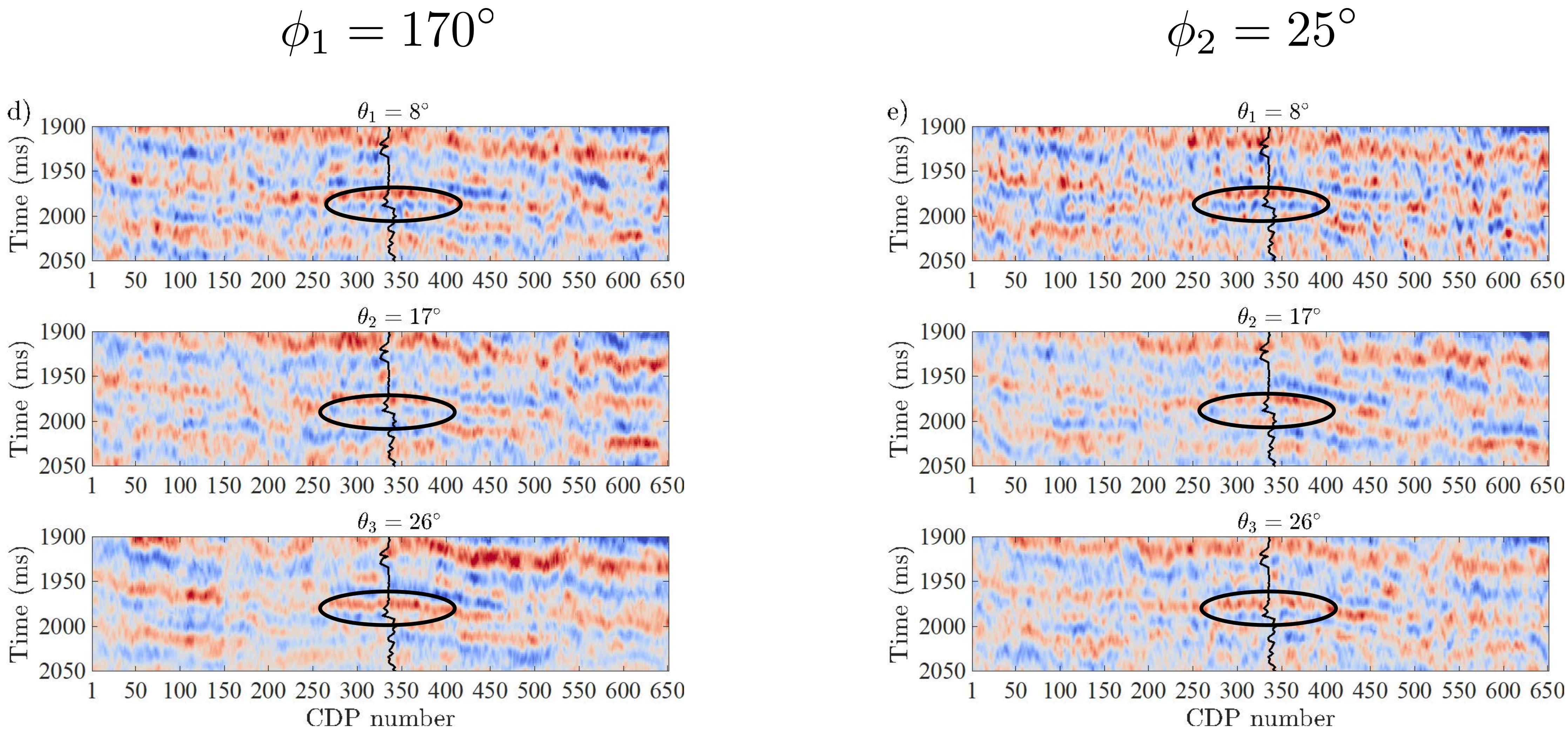

PS-wave stacked data of small, middle and large angles

Numerical examples

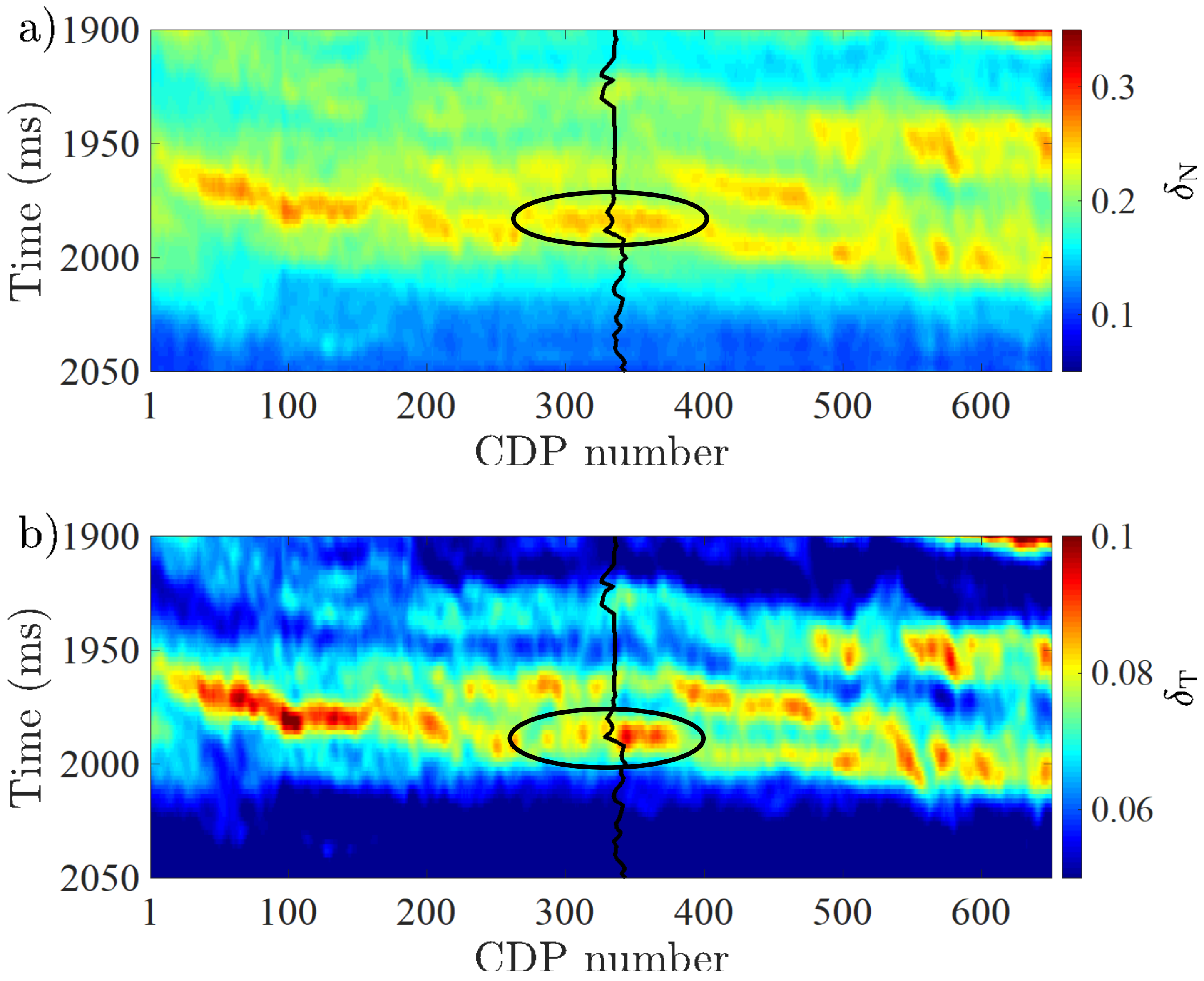

Conclusions

- We derive linearized PP- and PS-wave reflection coefficients in terms of two sets of fracture weaknesses to model how fracture connectivity affects reflection coefficients;
- We establish an inversion approach combining LS algorithm and Bayesian MCMC method to estimate fracture weaknesses from azimuthal seismic amplitudes;
- Tests on noisy synthetic data and real data reveal that the proposed approach is stable and robust and can provide the possibility to determine how fractures distribute and whether fractures are connected.

Acknowledgements

- CREWES sponsors
- Tongji University
- NSERC (CRDPJ 461179-13 and CRDPJ 543578-19)
- CREWES faculty, staff and students
- CNPC RIPED-Northwest for data use

Thank you